J|A|C|S COMMUNICATIONS

Published on Web 07/31/2009

# High-Affinity Peptide-Based Collagen Targeting Using Synthetic Phage Mimics: From Phage Display to Dendrimer Display

Brett A. Helms, Sanne W. A. Reulen, Sebastiaan Nijhuis, Peggy T. H. M. de Graaf-Heuvelmans, Maarten Merkx, and E. W. Meijer*

*Laboratory of Chemical Biology and Institute for Complex Molecular Systems, Eindhoven University of Technology, P.O. Box 513, 5600 MB Eindhoven, The Netherlands*

Received March 23, 2009; E-mail: E.W.Meijer@tue.nl

Collagens are extracellular matrix (ECM) proteins that provide mechanical strength to tissues and are important in cell attachment, differentiation, and migration.[1,2] Visualization of collagen networks in tissues is of great interest, particularly in light of the many human ailments that are characterized by ECM degradation or turnover such as angiogenesis, myocardial infarction, and atherosclerosis.[3,4] Naturally occurring collagen binding proteins such as the von Willebrand Factor (vWF) or CNA35[5−7] labeled with fluorescent dyes or collagen-specific antibodies[8] are frequently employed for collagen imaging. Protein-based targeting strategies have a few key limitations, however: tissue penetration depth decreases with increasing size, and naturally occurring collagen binding proteins are often promiscuous in binding to collagen's many subtypes, effectively reducing the structural information gleaned with these probes.[5,6] The use of short peptides as targeting ligands presents an attractive alternative: their activity often does not require folding, and their chemical synthesis is inexpensive in comparison to, e.g., antibodies.

Phage display has proven to be a particularly efficient method to rapidly screen large peptide libraries for targeting ligands to a broad variety of substrates.[9] Peptides derived from phage display, however, suffer from a serious drawback in that they typically show significantly weaker binding than their respective high affinity phage. This applies in particular to peptides targeting protein surfaces and results from the intrinsic flexible nature and limited binding interface of peptides.[10] For example, the WREPSFCALS peptide derived from vWF has been reported to bind bovine collagen type I with an apparent $K_d$ of only 100 $\mu$M.[11] In related work, Caravan et al. reported the development of a disulfide bond constrained collagen binding peptide, but its low $\mu$M affinity was obtained only after extensive affinity maturation via the incorporation of non-natural amino acids.[12,13]

As collagens and other ECM proteins have repetitive primary sequences and elaborate structural hierarchies permitting multivalent interactions with cells, a targeting strategy based on multivalent peptide binding is highly attractive. In fact, each phage in the widely used M13 libraries presents five peptide ligands fused to the N-terminus of the phage pIII coat protein at one end of the phage particle. Affinity selection of peptide ligands using these libraries might thus rely on not only the specific amino acid sequence displayed at the phage head but also their presentation in multiple copies capable of interacting with collagens in a multivalent fashion. While a large number of multivalent approaches have been disclosed in recent years, most of them are designed for structurally well-characterized targets such as bacterial toxins and lectins.[14,15] Here we report a multivalent approach to enhance the affinity of phage-display derived peptides through reconstruction of the phage's multivalent architecture using carefully designed dendritic wedges as synthetic multivalent scaffolds (Figure 1). The approach is

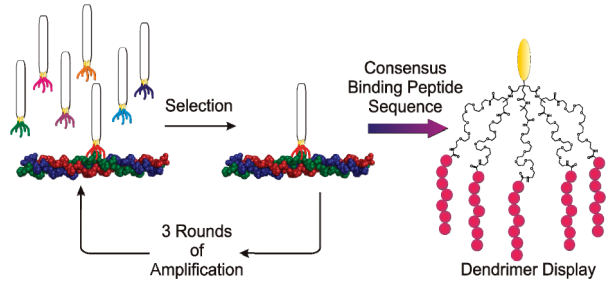


***Figure 1.*** From phage display to dendrimer display: phage display to collagen reveals a consensus binding sequence that is translated into a high affinity, versatile synthetic collagen-specific probe by mimicking the original pentavalent phage architecture on a dendritic wedge.

demonstrated using a collagen-specific 7-mer peptide sequence against rat tail collagen type I but is likely to be broadly applicable to other multivalent peptide or protein architectures.

Collagen binding phages were identified from commercially available M13 phage libraries containing linear 7-mer, linear 12-mer, or cyclic 7-mer peptides. Initially, strong background binding was observed between the phage and rat tail collagen type I coated on 96-well plates, probably due to Coulombic interactions between the polyanionic phage and the positively charged collagen. Screening of several buffer conditions revealed that this background binding was efficiently suppressed at 0.5 M NaCl. ELISA experiments showed clear enrichment with collagen binding phage for the linear 7-mer library after two rounds of panning, whereas little enrichment was observed for either of the other two libraries (Figure S1). Subsequent panning experiments were done with the linear 7-mer library using either low pH elution or competitive elution with the collagen binding protein CNA35. Highly homologous peptide sequences were obtained for all panning experiments with nearly all clones containing the consensus sequence H-V-F/W-Q/M-Q-P/A-P/K (Figure S1). This newly discovered consensus sequence is markedly different from any of the previously reported collagen binding peptides.[11,13,16] To mimic the multivalent peptide presentation on the M13 phage head, a pentavalent dendritic platform was constructed, which was designed to incorporate various imaging modalities at the focal point in addition to five copies of the collagen binding phage peptide (Scheme 1).

The branched core of the pentameric structure was built up via a double Michael addition of the bivalent acrylamide **10** to the linear nitroalkane **6** (Scheme 1 and Supporting Information). This $AB_5$ synthon is versatile, incorporating oligoethyleneglycol-based flexible linkers to peptide ligands at the periphery and nitro, biotin, or fluorescein moieties at the focal point of the wedge. Final construction of the collagen binding phage mimics was accomplished by native chemical ligation of $H_2N$-H(Dnp)-

10.1021/ja902285m CCC: $40.75 

***Scheme 1.*** Synthesis of Pentavalent Dendritic Wedges as Scaffolds for Phage Peptide Presentation[a]

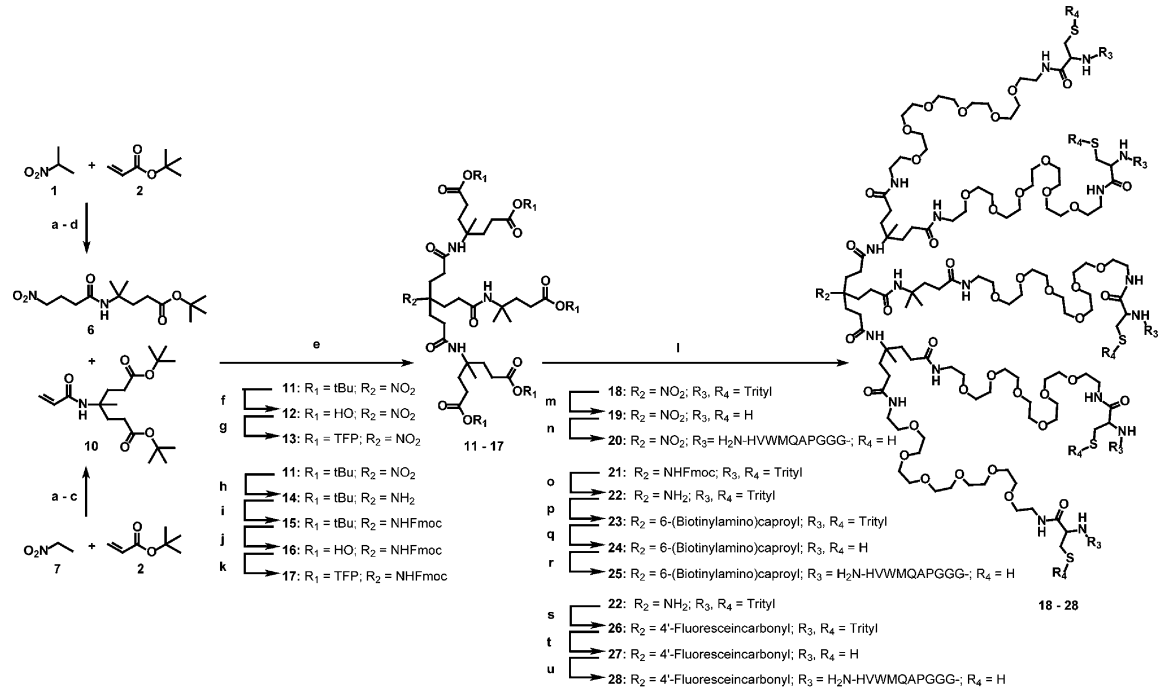


[a] For reaction conditions, see Figure S2.

VWMQAPGGG-MPAL thioesters to wedges bearing five N-terminal cysteines (**19**, **24**, and **27**). Complete conversion to the pentameric collagen binding constructs (**20**, **25**, and **28**) was observed after 16 h at 37 °C in the presence of benzyl mercaptan with thiophenol as the catalyst.[17]

The effect of multivalent display on collagen affinity was studied by ELISA assays using biotinylated monovalent and pentavalent constructs and substrates coated with rat tail collagen type I (Figure 2A). Monovalent $H_2N$-HVWMQAPGGGK(Biotin)-$NH_2$ yielded a $K_d = 61 \pm 5$ $\mu$M, while a scrambled or reversed sequence showed no significant binding above background. Titration experiments for the pentameric phage analogue **25** revealed a 100-fold improvement in collagen affinity, showing the same affinity ($K_d = 550 \pm 100$ nM) as that of the natural collagen protein CNA35. Moreover, the plot for **25** seems to show a more cooperative affinity—a more steep increase at the low concentration part of the titration—than a simple 1:1 Langmuir binding model (see Supporting Information). To understand how the increase in affinity is reflected in the association and dissociation kinetics, surface plasmon resonance (SPR) was employed. Not surprisingly, the monovalent peptide showed fast association and dissociation kinetics to rat tail collagen type I immobilized on a dextran-coated biosensor surface (Figure 2B). Association of the pentamer **20**, in contrast, was slower, possibly due to its larger size. The most dramatic effect of the pentamer manifests in its dissociation kinetics, where persistent adhesion of **20** to collagen was observed (Figure 2C). Low pH elution, similar to that used for the initial phage panning, was required to release the pentamer from the collagen-coated SPR surface. The enhancement in binding over 2 orders of magnitude between the free peptide and the peptide pentamer suggests that dendrimer display is capable of harnessing at least part of the favorable binding characteristics of the peptide-displaying phage.

The $AB_5$ dendritic wedge mimics several key features of the phage, including its overall valency and its conjugation of peptide ligands via their C-terminus. In this case, the collagen binding peptides are linked using a short GGG spacer and PEG chains that

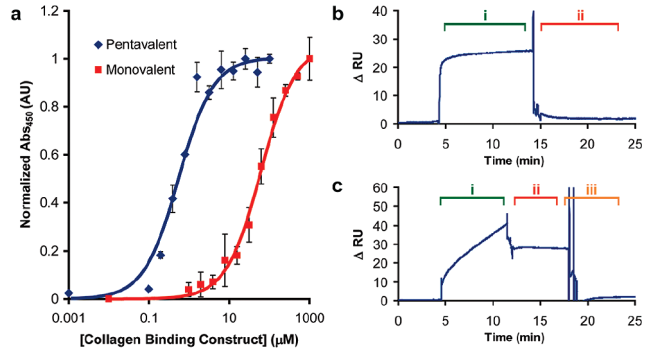


***Figure 2.*** Binding properties of pentavalent and monovalent collagen binding peptides. (a) Binding of biotinylated monovalent and pentavalent peptides to immobilized rat tail collagen type I was detected using HRP-conjugated antibiotin antibody. Solid lines represent fits to a 1:1 Langmuir binding model. (b/c) SPR analyses of the association (i) and dissociation (ii) kinetics of monovalent (b) and pentavalent (c) peptides binding to rat tail collagen type 1. Plots show reference subtracted responses obtained by flowing 1 mM $H_2N$-HVWMQAPGGGC-$NH_2$ (b) or 25 $\mu$M **20** (c) over CM5 chips immobilized with 5000 RU (b) and 1500 RU (c) of collagen type I. Conditions: HBS-EP buffer pH 7.4 with 1 mM DTT at 25 °C. Regeneration and re-equilibration (iii): 10 mM glycine pH 1.5 for 2 × 30 s then running buffer for 5 min.

together provide an average distance that is similar to the 2−3 nm spacing between two adjacent pIII domains on the phage. Unlike the peptides displayed on the phage, which are restricted by the pIII proteins, the peptide ligands on the dendritic wedge most likely assume a random coil conformation, acting independently in their interaction with collagen. For example, tryptophan fluorescence and circular dichroism experiments (Figures S17 and S18) did not show any evidence for the formation of secondary or tertiary structure upon multimerization of the collagen binding peptide onto the dendritic wedge. To provide a starting point for understanding the effect of multivalency in these systems, we analyzed the binding using the minimal model of a bivalent interaction. The enhanced affinity can be understood by assuming that binding of one peptide

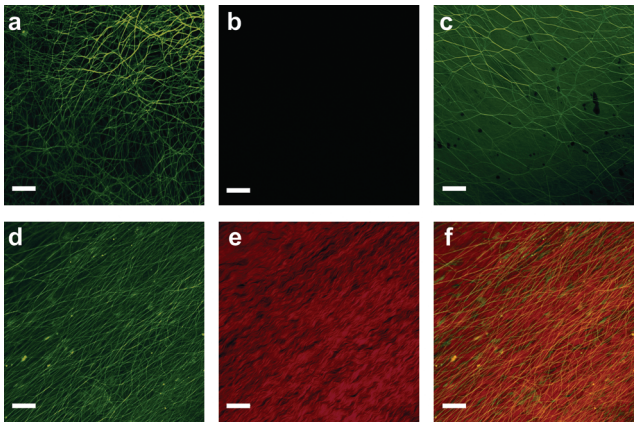


***Figure 3.*** Laser scanning confocal microscopy (LSCM) images of 1 × 1 cm porcine pericardium sections showing the performance of dendrimer-displayed collagen binding peptides in the ex vivo imaging of collagen in native tissue. Tissues were incubated for 3 h in HBS pH 7.4 with 0.6 $\mu$M **28** (a) or $H_2N$-HVWMQAPGGGK(fluorescein)-$NH_2$ at concentrations of 0.6 $\mu$M (b) and 60 $\mu$M (c). (d−f) Costaining of a tissue section with 6 $\mu$M AlexaFluor568-labeled CNA35 in HBS pH 7.4 for 3 h, followed by 0.6 $\mu$M **28** for an additional 2 h (d: green channel showing **28**: e: red channel showing AlexaFluor568-labeled CNA35; f: overlay of green and red channels). The scale bar represents 50 $\mu$m.

ligand increases the effective molarity (EM) to 0.34 ± 0.07 mM for binding to a second receptor site.[18] This number is consistent with the length of the flexible linker used here and an average distance of ∼30 Å between two peptide binding sites.[19] This analysis also indicates that multivalent binding is only effective when EM > $K_{inter}$ and that statistical factors contribute to enhance the effect of multivalent interactions. A more detailed characterization of the binding specificity of phage peptide dendrimers and its dependency on the molecular architecture, valency of the wedge, and density of binding sites is ongoing.

Having established the favorable binding characteristics of the phage mimics on collagen-coated substrates in vitro, we next assessed their efficacy for selective collagen staining in the more heterogeneous environment of native collagen-containing tissues. We tested the performance of fluorescein-labeled monomers and pentamers for collagen imaging in the parietal pericardium, a fibrous sac around the heart that consists mainly of collagen type I and some type III.[20,21] Incubation of pig parietal pericardium with 0.6 $\mu$M fluorescein-labeled peptide pentamer **28** showed a distinct fibrous network with fibers of an ∼2 $\mu$m thickness (Figure 3). Consistent with the *in vitro* binding studies, no collagen was detected using the same concentration of the monovalent collagen binding peptide. Similar collagen architectures as observed for the pentamer at 0.6 $\mu$M were observed when using 60 $\mu$M of the monovalent peptide, but the amount of background fluorescence was significantly increased. To compare the properties of the peptide pentamer to those of CNA35, the same tissue was costained with 0.6 $\mu$M **28** (green) and 6 $\mu$M AlexaFluor568-labeled CNA35 (red). Both probes visualize collagen fibers oriented in the same direction, but a more specific stain was observed for the peptide pentamer compared to CNA35 (Figure 3D−F). The wave-like collagen structures observed with the CNA35 agree with other imaging studies of total collagen content in pericardial tissues.[22] These results are thus consistent with previous findings that CNA35 actually binds to various types of collagen with similar affinity[6] and suggest that phage display is a suitable approach to identify more specific targeting ligands.[23]

In summary, the $AB_5$ dendritic wedge represents a well-defined, highly versatile platform for the affinity enhancement of phage-display derived peptides by mimicking key aspects of the multivalent architecture of the phage head. The collagen targeting ligands presented here provide attractive alternatives for antibody- and protein-mediated targeting of collagen remodeling in a number of disease processes. These results thus emphasize the advantage of combining the strength of biological display methods for the affinity selection of peptide ligands with the ability of synthetic chemistry to provide a wide variety of functional groups and 3D topologies.

**Acknowledgment.** We thank Katy Nash Krahn, Ingrid van Baal, Tilman Hackeng (Maastricht), and Jos Raats (Nijmegen) for experimental support. This work was supported by NWO VIDI Grant 700.56.428 to M.M., a SPINOZA grant to E.W.M., and the BSIK Program BSIK03033.

**Supporting Information Available:** Experimental details regarding phage display, dendrimer and peptide synthesis, *in vitro* binding experiments, and collagen imaging. This material is available free of charge via the Internet at http://pubs.acs.org.

## References

(1) Even-Ram, S.; Yamada, K. M. *Curr. Opin. Cell Biol.* **2005**, *17*, 524–532.
(2) Gelse, K.; Poschl, E.; Aigner, T. *Adv. Drug Delivery Rev.* **2003**, *55*, 1531–1546.
(3) Adiguzel, E.; Ahmad, P. J.; Franco, C.; Bendeck, M. P. *Vasc. Med.* **2009**, *14*, 73–89.
(4) Myllyharju, J.; Kivirikko, K. I. *Ann. Med.* **2001**, *33*, 7–21.
(5) Boerboom, R. A.; Krahn, K. N.; Megens, R. T.; van Zandvoort, M. A.; Merkx, M.; Bouten, C. V. *J. Struct. Biol.* **2007**, *159*, 392–399.
(6) Krahn, K. N.; Bouten, C. V.; van Tuijl, S.; van Zandvoort, M. A.; Merkx, M. *Anal. Biochem.* **2006**, *350*, 177–185.
(7) Megens, R. T.; Oude Egbrink, M. G.; Cleutjens, J. P.; Kuijpers, M. J.; Schiffers, P. H.; Merkx, M.; Slaaf, D. W.; van Zandvoort, M. A. *Mol. Imaging* **2007**, *6*, 247–260.
(8) Hayes, A. J.; Hughes, C. E.; Caterson, B. *Methods* **2008**, *45*, 10–21.
(9) Smith, G. P.; petrenko, V. A. *Chem. Rev.* **1997**, *97*, 391–410.
(10) Sergeeva, A.; Kolonin, M. G.; Molldrem, J. J.; Pasqualini, R.; Arap, W. *Adv. Drug Delivery Rev.* **2006**, *58*, 1622–1654.
(11) Takagi, J.; Asai, H.; Saito, Y. *Biochemistry* **1992**, *31*, 8530–8534.
(12) Caravan, P.; Das, B.; Deng, Q.; Dumas, S.; Jacques, V.; Koerner, S.; Kolodziej, A.; Looby, R. J.; Sun, W. C.; Zhang, Z. *Chem. Commun.* **2009**, 430–432.
(13) Caravan, P.; Das, B.; Dumas, S.; Epstein, F. H.; Helm, P. A.; Jacques, V.; Koerner, S.; Kolodziej, A.; Shen, L.; Sun, W. C.; Zhang, Z. *Angew. Chem., Int. Ed.* **2007**, *46*, 8171–8173.
(14) Choi, S.-K. *Synthetic multivalent molecules. Concept and biomedical applications*; Wiley: Hoboken, NJ, 2004.
(15) Kitov, P. L.; Sadowska, J. M.; Mulvey, G.; Amstrong, G. D.; Ling, H.; Pannu, N. S.; Read, R. J.; Bundle, D. R. *Nature* **2000**, *403*, 669–672.
(16) Depraetere, H.; Viaene, A.; Deroo, S.; Vauterin, S.; Deckmyn, H. *Blood* **1998**, *92*, 4207–4211.
(17) van Baal, I.; Malda, H.; Van Dongen, J. L. J.; Merkx, M.; Meijer, E. W.; Synowsky, S. A.; Hackeng, T. M. *Angew. Chem., Int. Ed.* **2005**, *44*, 5052–5057.
(18) Krishnamurthy, V. M.; Semetey, V.; Bracher, P. J.; Shen, N.; Whitesides, G. M. *J. Am. Chem. Soc.* **2007**, *129*, 1312–1320.
(19) van Dongen, E. M. W. M.; Evers, T. H.; Dekkers, L. M.; Meijer, E. W.; Klomp, L. W. J.; Merkx, M. *J. Am. Chem. Soc.* **2007**, *129*, 3494–3495.
(20) Keene, D. R.; Sakai, L. Y.; Bachinger, H. P.; Burgeson, R. E. *J. Cell Biol.* **1987**, *105*, 2393–2402.
(21) Simionescu, D.; Iozzo, R. V.; Kefalides, N. A. *Matrix* **1898**, *9*, 301–310.
(22) Rodriguez-Feo, J. A.; Sluijter, J. P. G.; de Kleijn, D. P. V.; Pasterkamp, G. *Curr. Pharm. Des.* **2005**, *11*, 2501–2514.
(23) Lusvarghi, S.; Kim, J. M.; Creeger, Y.; Armitage, B. A. *Org. Biomol. Chem.* **2009**, *7*, 1815–1820.

JA902285M